



Some Organic Compounds as Accelerator and Inhibitor for Electroplating Process

ABDEL-MONEM M. AHMED¹, AHMED F. EL ADL^{2*} and S.M. SELEIM¹

¹Department of Chemistry, Faculty of Science, Alexandria University, Alexandria, Egypt

²Egyptian Environmental Affairs Agency, Alexandria, Egypt

*Corresponding author: E-mail: ahmedeladl@live.com

(Received: 9 August 2012;

Accepted: 27 May 2013)

AJC-13553

The electroplating of copper on copper and steel surface was studied in absence and in presence of 6(2, 4-dimethoxyphenyl)-2-oxo-1,2,3,4-tetrahydropyrimidine-5-carbonitrile [Compound I] and calcium bis-[(R)-3-(2, 4-dihydroxy-3, 3-dimethylbutyramido) propionate] (D-calcium pantothenate) [compound II] by measuring the limiting current. It is found that, the rate of plating depends on the concentration of CuSO₄, types of organic additives and its concentrations, viscosity, density and types of cathode. It is found that the rate of electroplating increases by increase of concentration in case of electroplating of copper. The percentage of acceleration range from 15 to 60 % depend on organic additives and its concentration. In case of electroplating of steel the rate of deposition decreases and the percentage of inhibition ranged from 11.8 to 35.3 % depending on the type of organic additives and its concentrations. Langmuir and kinetic adsorption isotherm were studied.

Key Words: Electroplating, Inhibition, Acceleration, Copper, Steel, Limiting current, Mass transfer.

INTRODUCTION

Copper electrodeposition plays a key role in the electronic industry, particularly for printed circuit manufacture and for circuit interconnection where the filling of trenches with a conducting material on the micro and sub-microscale with a depth/width ratio up to 10 is required¹⁻³. Copper chip interconnection technology was developed about two decades ago^{4,5}, significantly improving the conductance of integrated device connections. For this purpose, copper electrodeposition plating baths utilize a mixture of organic and inorganic additives that obviously increases the complexity of these systems and the reactions occurring there in. Consequently, this fact makes the molecular interpretation of these processes, based upon possible interactions of the growth front with the various constituents in the plating solutions, more difficult.

Commonly, the presence of additives in metal plating solutions produces a better leveling effect at the electrodeposits surface as additives distinctly influence the electrodeposition rate at protrusions and recesses^{6,7}. Additives may also affect the diffusion of reactants from the bulk of the solution towards the reaction front by changing the plating solution properties and the surface diffusion of metal ad-ions or ad-atoms to stable lattice sites. Furthermore, the preferential adsorption of either additives or their derivatives on surfaces with diverse curvature may assist the electrodeposition rate⁸.

The concentration of Cu(I) species would be enhanced inside trenches due to the decrease in the concentration of dissolved oxygen there as compared to planar surfaces⁹. However, most accepted kinetic models assume the preferred adsorption of the accelerant at the bottom of trenches^{7,10} and its accumulation is assisted by the simultaneous decrease in surface area caused by metal electrodeposition inside trenches¹⁰. Other models suggest that the inhibitor, *i.e.*, the large PEG-chloride ion adsorbate, blocks the electrodeposition process at the trench entrance, whereas the smaller accelerant species, *i.e.*, MPSA-chloride complex, reaches the trench bottom producing a bottom-up electrodeposition¹¹. Although these theories should be considered important contributions to the mechanism of the above processes. Further knowledge about the interaction of intervening species both among them and with the growing copper phase is required.

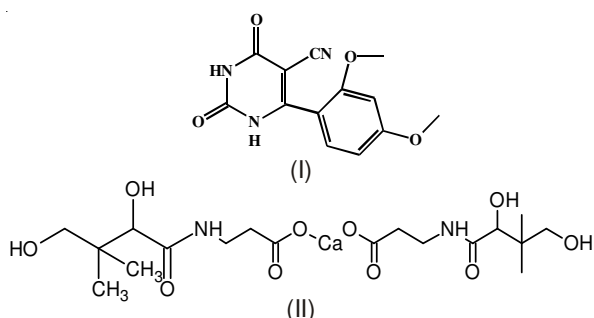
In modern electrodeposition practice, it is well known that the addition of even small amounts of certain substances leads to significant changes in the properties and aspect of the deposition^{12,13}.

Recent reviews have tried to summarize their different effects. Levelers have the ability to produce deposits relatively thick in small recesses and relatively thin on small protrusions. They act by adsorption at points where otherwise there would be a rapid deposition of the metal³⁻⁸.

Previous studies have shown that reduced the limiting current of uranium⁹ and manganese¹⁰ deposit from phosphoric acid and mercury cathode. The object of this work is to study the effect of some organic compounds additives on electroplating of steel and copper.

EXPERIMENTAL

Melting points were determined using a Kofler block instrument. IR spectra were recorded with a Perkin-Elmer model 1720 FTIR (KBr), ¹H NMR spectra were recorded with Bruker AC 250 FT NMR spectrometer at 250 MHz with TMS as an internal standard. MALDI-MS were measured with a KRATOS Analytical Compact, using 2,5-dihydroxybenzoic acid (DHB) as matrix. The (M+ Na)⁺ ions were peak-matched using ions derived from the 2,5-dihydroxybenzoic acid matrix. The microanalyses were performed at the microanalytical unit, Cairo University, Egypt and were found to agree favourably with the calculated values. Analar graded CuSO₄·5H₂O and H₂SO₄ (98 % w/w), supplied by BDH Chemicals Ltd., were used for the preparation of the electrolytes. (Scheme-I)



Compound I: 6-(2,4-dimethoxyphenyl)-2-oxo-1,2,3,4-tetrahydropyrimidine-5-carbonitrile; **Compound II:** Calcium bis-[(R)-3-(2,4-dihydroxy-3,3-dimethylbutyramido) propionate] (D-calcium pantothenate)

Scheme-I: Structures of compounds

Cell and circuit

Using rectangular electrode: The cell consisted of a rectangular plastic container (5.1 cm × 5 cm × 10 cm) with electrode fitting the whole cross section area, the anode was rectangular copper sheet (10 cm height and 5 cm width); the cathode was steel sheet with an inter-electrode distance of 5 cm. The electrical circuit consists of 6 volt d.c. power supply connected in series with cell along with a rheostat and multi-range ammeter. A voltmeter is connected in parallel with the cell to measure the voltage (Figs. 1 and 2).

Using rotating cylinder electrode: The anode consisted of Cu metal cylinder 1 cm diameter and 5 cm length, the unexposed area of the cylinder is covered by epoxy resin. The anode was made from cylindrical copper metal counter electrode of 12 cm diameter. It acted as the reference electrode by virtue of its high surface area compared to that of anode.

RESULTS AND DISCUSSION

Fig. 3 shows the cathodic polarization curve for copper electroplating from sulphate solution in presence of compound I in case of Cu-Cu as example. Those curve were used to calculate limiting current and mass transfer coefficient.

$$K = I_l / zFC_o$$

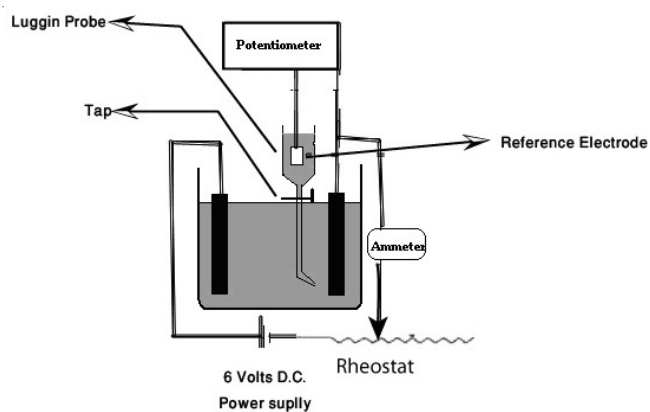


Fig. 1. Electrolytic cell and the electrical circuit showing the position of the two parallel vertical plates and the reference electrode. The ammeter connected in series, while the potentiometer in parallel

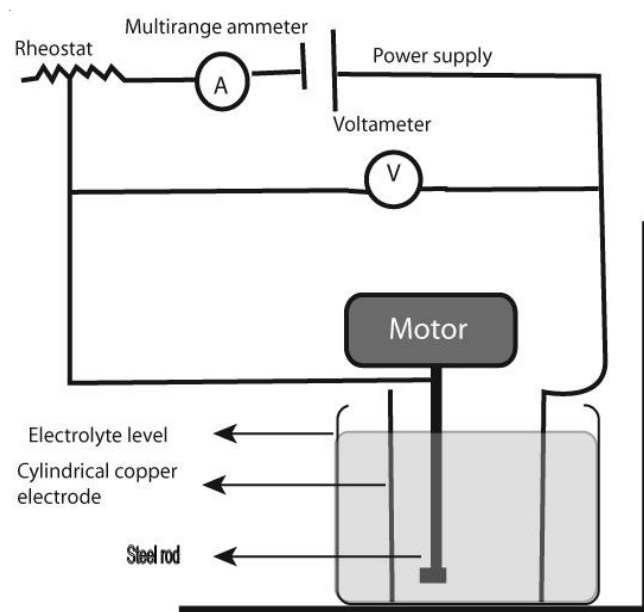


Fig. 2. Electrolytic cell and the electrical circuit using rotating cylinder electrode

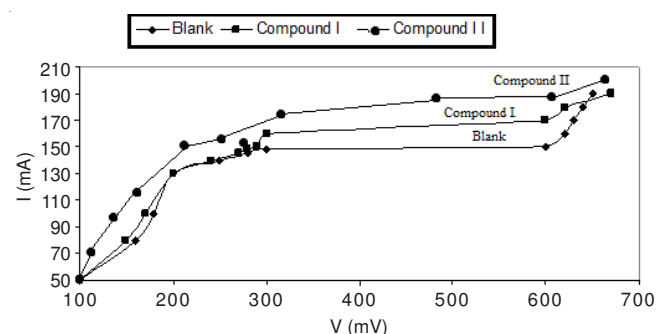


Fig. 3. Relation between current and volt for blank solution and in presence of all organic compounds at 25 °C in case of copper-copper cell

where I_l is limiting current (mA), z is valance, F is Faraday's constant and C_o is the bulk concentration of CuSO₄ (mol.cm⁻³).

Effect of concentration of CuSO₄ on the limiting current: Table-1 and Figs. 4 and 5 give the effect of copper sulphate concentration at the limiting current at 25 °C and 10 cm height in case of copper-copper as well as copper-steel. It is obvious that I_l increases by increasing copper sulphate concentration.

TABLE-1
LIMITING CURRENT IN ABSENCE AND PRESENCE
OF ORGANIC ADDITIVES AT 25 °C

Organic additives	C. 10 ⁴ (mol L ⁻¹)	I _l (mA)	
		Copper-steel	Copper-copper
Compound I	0	180	200
	1.5	150	230
	2.9	145	240
	4.4	140	250
	5.9	130	260
	7.3	120	265
	8.8	115	270
	10.0	110	270
Compound II	0	180	200
	0.84	150	230
	1.7	140	250
	2.5	135	260
	3.4	145	270
	4.2	140	275
	5.0	135	280
	5.9	130	320

TABLE-2
RELATION BETWEEN PERCENTAGE ACCELERATION
AND CONCENTRATION AT 25 °C IN PRESENCE
OF COPPER CATHODE

Organic additives	C. 10 ⁴ (mol L ⁻¹)	I _b (mA)	I _l (mA)	Acceleration (%)
Compound I	1.5	200	230	15
	2.9	200	240	20
	4.4	200	250	25
	5.9	200	260	30
	7.3	200	265	33
	8.8	200	270	35
	10	200	270	35
	Compound II	0.84	200	230
1.7		200	250	25
2.5		200	260	30
3.4		200	270	35
4.2		200	275	38
5		200	280	40
5.9		200	320	60

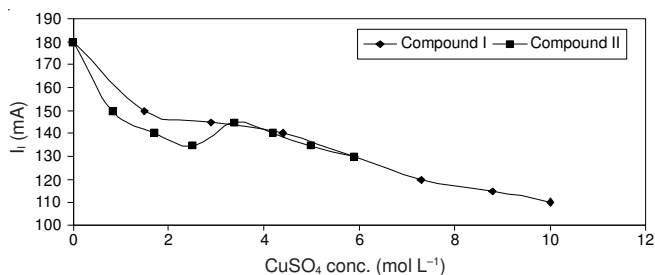


Fig. 4. Effect of copper sulphate concentration at the limiting current at 25 °C in case of copper-steel cell

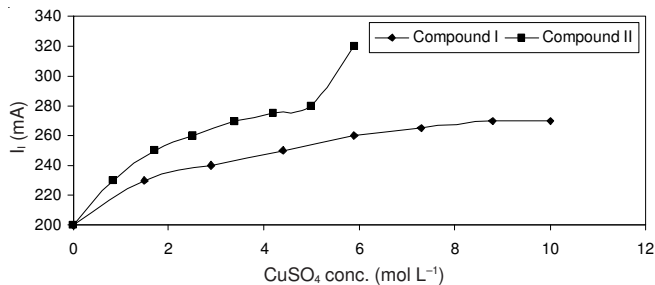


Fig. 5. Effect of copper sulphate concentration at the limiting current at 25 °C in case of copper-copper cell

Increasing the CuSO₄ content in the bath decreases the cathodic polarization and increases the limiting current plateau. These results were expected due to an increase in the relative abundance of the uncomplexed Cu²⁺ ions in the solution.

Effect of the concentration of organic additives on the electroplating current

In presence of copper-copper: The observed limiting current, represents the rate of deposition of copper metal in acidified CuSO₄ solution at 25 °C. It was found that the limiting current increased with increasing the concentration of organic compound additives. Table-2 and Fig. 6 show the dependence of current on the concentration of organic compound additives. It was found that the limiting current increased with increasing the concentration of organic compound. From the practical point of view, it is recommended on the basis of the results that, it may use relatively high organic additives percentage to accelerate the plating or deposition of metal.

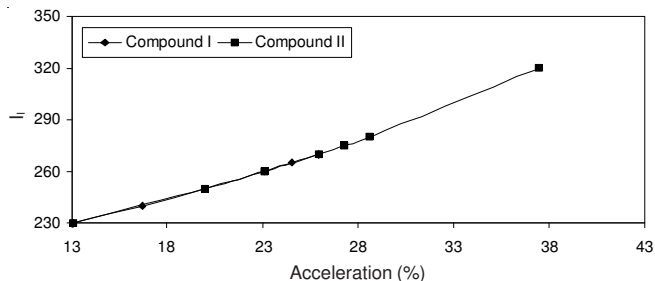


Fig. 6. Effect of organic additives concentrations on limiting current in presence of copper-copper cell

If the limiting current in absence of organic compound is I and in the presence of organic compound is I_l the percentage of acceleration can be calculated from the following equation:

$$\% \text{ acceleration} = [(I_l - I_b)/I_l] \times 100$$

Table-2 and Fig. 6 showed that the acceleration per cent and caused by organic compound ranged from 1.4 to 50 depending on the type of organic additives and its concentration in case of all additives used.

The limiting current increases with increasing the concentration of additives, this is in contrast with the finding of other authors who worked within the same range of concentration used other anode geometries^{14,15}.

An explanation for the increase of the rate of deposition may be due to that water molecules bounded by a hydrogen bond to an acid are less nucleophilic than water molecules bounded by a hydrogen bond with each other¹⁶⁻²².

The rate of electrodeposition is in contrast to that reported by other authors²³⁻²⁷. The increase in mass transfer coefficient or the rate of electrodeposition is attributed to additives decrease the local solution viscosity at anode surface with a consequent increase in the diffusivity of copper ion and the increase in the rate of deposition with increasing the concentration of additives, which is attributed to those molecules accelerate the natural convection flow arising from the density difference between bulk solution and solution at electrode surface²⁸.

Rate of electrodeposition and the limiting current is observed to increase in the presence of electrolyte or additives probably due to the increase of the conductivity of solution

mixture in the presence of organic additives, the limiting current is found to be higher in presence of organic additives add to solution than in absence of organic additives.

The increase of rate will depend on the organic additives composition and its structures the protolytic action and oxygen solubility.

It is found that the rate of electrodeposition increases in the following order: calcium *bis*-[(R)-3-(2, 4-dihydroxy-3,3-dimethylbutyramido) propionate] (D- calcium pantothenate) [compound II] > 6(2, 4-dimethoxyphenyl)-2-oxo-1,2,3,4-tetrahydropyrimidine-5-carbonitrile [compound I].

This compound has more O group which make as barrier of Cu^{2+} and compound I.

In presence of copper-steel: The limiting current in absence of organic compound (I_b) and in presence of organic compound I_c , is related to the percentage of inhibition by the equation:

$$\% \text{ inhibition} = [(I_b - I_c)/I_b] \times 100$$

Table-3 and Fig. 7 showed that the % Inhibition caused by organic compounds which ranged from 1.89 to 35.85 % for cell using copper anode.

Organic additives	C. 10^4 (mol L ⁻¹)	I_b (mA)	I_c (mA)	Inhibition (%)
Compound I	1.5	170	150	11.8
	2.9	170	145	14.7
	4.4	170	140	17.6
	5.9	170	130	23.5
	7.3	170	120	29.4
	8.8	170	115	32.4
	10	170	110	35.3
Compound II	0.84	170	150	11.8
	1.7	170	140	17.6
	2.5	170	135	20.6
	3.4	170	145	14.7
	4.2	170	275	38
	5	170	280	40
	5.9	170	320	60

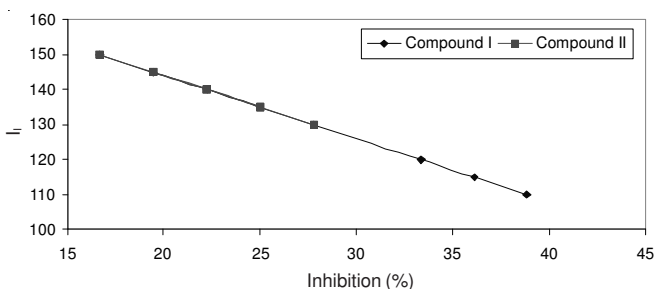


Fig. 7. Effect of organic additives concentrations on limiting current in presence of copper-steel cell

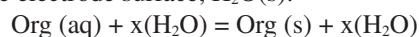
The percentage inhibition was calculated depending on the concentration and type of inhibitor. It is observable that percentage inhibition increased as concentration increased.

The results show that the presence of organic compound has an inhibiting effect on the kinetics of the copper discharge process, pointed out by the decrease of the exchange current

density. The inhibition enhancing due to increasing the organic compound concentration could be related to the strong adsorption of organic compound constituents on the copper electrode surface, which is in agreement with the decay of the current intensity observed on the polarization curves.

The presence of organic compound changes the mechanism of the copper electrodeposition as it can be seen from the decreasing of the cathodic transfer coefficient. A possible explanation for this fact consists in the increasing role of an additional reaction that produces the same chemical species Cu^+ as those involved in the rate determining reaction²⁰.

Adsorption isotherm: The electrochemical processes on the metal surface are likely to be closely related to the adsorption of the inhibitor²¹ and the adsorption is known to depend on the chemical structure of the inhibitor²²⁻²⁴. The adsorption of the inhibitor molecules from aqueous solutions can be regarded as (quasi-substitution) process²² between the organic compound in the aqueous phase, Org. (aq) and water molecules at the electrode surface, $\text{H}_2\text{O}(s)$:



where x (the size ratio) is the number of water molecules displaced by one molecule of organic inhibitor. Adsorption isotherms are very important in determining the mechanism of organo-electrochemical reactions.

The most frequently used isotherms are those of Langmuir, Frumkin, Parsons, Temkin, Flory-Huggins and Bockris-Swinkels²⁵⁻²⁷. All these isotherms are of the general form:

$$f(\theta, x) \exp(-a\theta) = KC$$

where $f(\theta, x)$ is the configuration factor depends essentially on the physical model and assumptions underlying the derivation of the isotherm²⁸. The mechanism of inhibition of reaction is generally believed to be due to the formation and maintenance of a protective film on the metal surface²⁹.

Inhibitor adsorption characteristics can be estimated by using the Langmuir isotherm given as³⁰:

$$KC = \theta/(1-\theta)$$

where K is the equilibrium constant of adsorption process, C is the concentration and θ is the surface coverage.

The degree of surface coverage θ at constant temperature was determined from³¹.

$$\theta = (I_b - I_c) / I_b$$

A plot of $[\theta/(1-\theta)]$ vs. (C) should yield straight line, Table-4 and Fig. 8 shows straight line indicating that all the inhibitors verify Langmuir adsorption isotherm.

Effect of stirring and applications of dimensional analysis: The effect of the speed of rotation on the rate of metal deposition can also be used to determine whether the electrodeposition process is diffusion controlled or chemically controlled process. If the rate of deposition increases by increasing the speed of rotation, then the reaction is diffusion controlled. However, if the rate of deposition is depend of the rotation, so the reaction is likely to be chemically controlled.

The angular velocity, ω , is given by:

$$\omega = (2\pi \text{ rpm})/60$$

Fig. 9 shows the relation between the limiting current density and the angular velocity; ω at different compositions of additives at different temperatures as representative graphs. Straight lines were obtained and the limiting current density

Organic additives	C. 10^4 (mol L ⁻¹)	θ	$\theta/1-\theta$	C/ $\theta \times 10^4$	log $\theta/1-\theta$
Compound I	1.5	0.12	0.13	12.5	-0.89
	2.9	0.15	0.17	19.3	-0.77
	4.4	0.18	0.21	24.4	-0.68
	5.9	0.24	0.31	24.6	-0.51
	7.3	0.29	0.42	25.2	-0.38
	8.8	0.32	0.48	27.5	-0.32
Compound II	0.84	0.12	0.13	7.0	-0.89
	1.7	0.18	0.21	9.4	-0.68
	2.5	0.21	0.26	11.9	-0.59
	3.4	0.15	0.17	22.7	-0.77
	4.2	0.18	0.21	23.3	-0.68
	5.0	0.21	0.26	23.8	-0.59
	5.9	0.24	0.31	24.6	-0.51

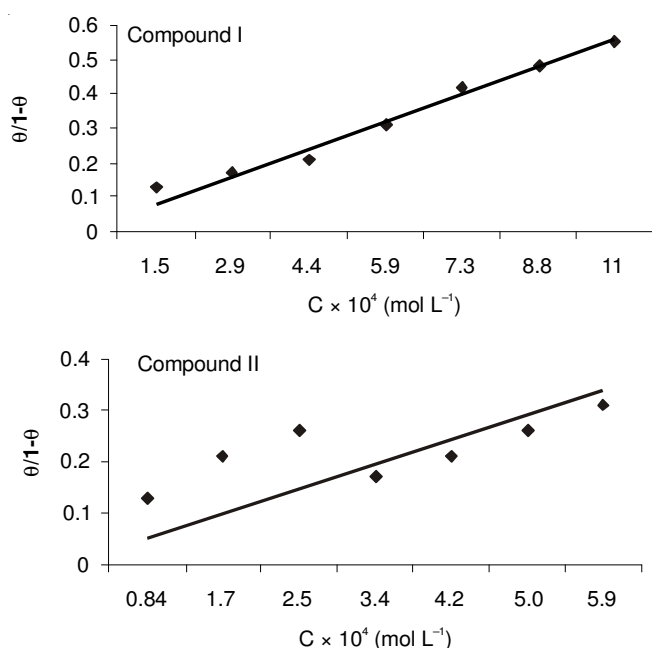


Fig. 8. Relation between $[\theta/(1-\theta)]$ vs. C for all compounds at 25 °C for steel cathode

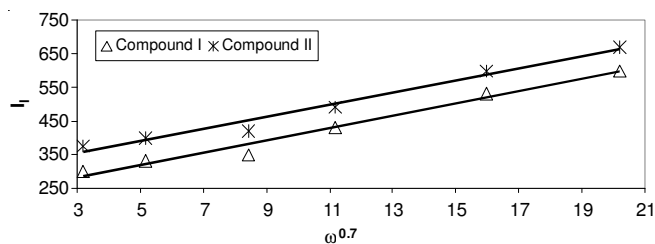


Fig. 9. Relation between limiting current (I_L) and $\omega^{0.7}$ for all organic additives at 25 °C

increases by increasing rotation, which indicates that the electrodeposition reaction in both cases, copper and lead anodes, is a diffusion controlled process.

Fig. 8 shows the effect of the speed of rotation on the limiting current density in presence of acids. The data satisfied the Eisenberg equation²⁹.

The diffusion coefficient of Cu^{2+} ions, D, in different solutions was determined from the values of limiting current densities using Eisenberg equation:³⁰

$$I_L = 0.07zFC_bU^{0.7}d_1^{-0.3}v^{-0.344}D^{0.644}$$

where, n is the number of exchanged electrons, F is Faraday's constant nF is called Faradic equivalence, C_b is the bulk concentration (mol cm⁻³), U is the peripheral velocity = ωr in cm rad.s⁻¹ (where, ω is the angular velocity and in rad.s⁻¹, r is the radial distance in cm) or $U = 2\pi \omega r$ in cm s⁻¹, d is the characteristic length for the rotating cylinder = the diameter of the cylinder in cm, D is the diffusion coefficient for the metal ions (Cu^{2+} ions in our case) in cm²s⁻¹ and ν is the kinematics viscosity in Stoke ($\nu = \eta/\rho$).

Values of D and ν for all solutions under different conditions are also recorded in Tables 5 and 6. The diffusion coefficient, D of Cu^{2+} ions in solutions containing additives decreases due to the increase in the viscosity η in accordance with the Stokes-Einstein equation³¹.

$$\eta D/T = \text{const}$$

where η is viscosity of solution (g.cm⁻¹.s⁻¹), D is the diffusion coefficient for the Cu^{2+} ions (cm²s⁻¹) and T is the absolute temperature (K).

The dimensionless groups Sh, Sc and Re used in convective mass transfer are³².

$$\text{Sherwood number: } (Sh = kd/D)$$

$$\text{Schmidt number: } (Sc = \nu/D)$$

$$\text{Reynolds number: } (Re = Ud/\nu)$$

where k = mass transfer coefficient, sec⁻¹; D = diffusion coefficient, cm²sec⁻¹; d = radius of cylinder, cm; ν = Kinematic viscosity; U = cylinder linear velocity ($U = \omega r$).

Reynolds number was used in forced convection problem, while Groasshof number was used in the case of natural of dimensional analysis.

To obtain an overall mass transfer correlation the present conditions by using the method of dimensional analysis, it is supposed that:

$$Sh = a(Re)^b(Sc)^{0.33}$$

a, b are constants.

By plotting log Sh/(Sc)^{0.33} against log Re, a straight line is obtained, its slope gives the constant (b) while the intercept gives the other constant (a) and (c) = 0.33 (indication forced convection).

Fig. 10 shows the overall mass transfer correlation for all organic compounds.

Table-7 summarizes the values of dimensional groups Sh, Sc and Re the used in obtained the correlation.

Organic additives	Copper cylinder	Steel cylinder
Blank	$Sh = 0.315 Re^{0.71} Sc^{0.33}$	$Sh = 0.500 Re^{0.539} Sc^{0.33}$
Compound I	$Sh = 0.268 Re^{0.7} Sc^{0.33}$	$Sh = 0.512 Re^{0.503} Sc^{0.33}$
Compound II	$Sh = 0.268 Re^{0.7} Sc^{0.33}$	$Sh = 0.471 Re^{0.530} Sc^{0.33}$

Fig. 10 shows that the data could be correlated by the following equations. For 6(2, 4-dimethoxyphenyl)-2-oxo-1, 2, 3, 4-tetrahydropyrimidine-5-carbonitrile [Compound I]:

$$\text{Copper cylinder } Sh = 0.268 Re^{0.7} Sc^{0.33}$$

$$\text{Steel cylinder } Sh = 0.512 Re^{0.503} Sc^{0.33}$$

For calcium bis-[(R)-3-(2, 4-dihydroxy-3, 3-dimethylbutyramido)propionate] (D-calcium pantothenate) [Compound II]:

TABLE-5
GENERAL CORRELATION OF FREE CONVECTION MASS TRANSFER FOR 6(2,4-DIMETHOXYPHENYL)-
2-OXO-1,2,3,4-TETRAHYDROPYRIMIDINE-5-CARBONITRILE (COMPOUND I)

$C \times 10^4$ (mol L ⁻¹)	rpm	T (°C)	I_1 mAcm ⁻²	$v \times 10^4$ (cm ² .sec ⁻¹)	$D \times 10^5$ (cm ² .sec ⁻¹)	Re	Sc	Sh	
4.4	50	25	330	8.64	2.87	1643	388	211	
		30	350			1643	368	200	
		35	380			1643	344	187	
		40	410			1643	316	171	
	100	25	350			1.48	3287	753	409
		30	370			1.56	3287	714	388
		35	390			1.56	3287	714	388
		40	420			1.73	3287	644	350
	300	25	430			0.62	9860	1798	975
		30	460			0.66	9860	1689	916
		35	480			0.65	9860	1715	930
		40	500			0.69	9860	1615	877
	500	25	530			0.49	16434	2275	1234
		30	570			0.53	16434	2103	1141
		35	600			0.53	16434	2103	1141
		40	610			0.54	16434	2064	1120
	700	25	600			0.41	23007	2718	1475
		30	630			0.43	23007	2592	1407
		35	650			0.42	23007	2654	1440
		40	660			0.42	23007	2654	1440

TABLE-6
GENERAL CORRELATION OF FREE CONVECTION MASS TRANSFER FOR CALCIUM BIS-[(R)-3-(2, 4-DIHYDROXY-3,
3- DIMETHYLBUTYRAMIDO) PROPIONATE] (D- CALCIUM PANTOTHENATE) (COMPOUND II)

$C \times 10^4$ (mol L ⁻¹)	rpm	T (°C)	I_1 mAcm ⁻²	$v \times 10^4$ (cm ² .sec ⁻¹)	$D \times 10^5$ (cm ² .sec ⁻¹)	Re	Sc	Sh	
2.5	50	25	400	8.98	3.9	1714	274	161	
		30	430			1714	256	150	
		35	450			1714	258	152	
		40	470			1714	245	144	
	100	25	420			1.97	3428	542	319
		30	450			2.11	3428	506	298
		35	460			2.01	3428	532	313
		40	480			2.12	3428	504	297
	300	25	490			0.76	10284	1406	827
		30	510			0.78	10284	1370	806
		35	530			0.76	10284	1406	827
		40	550			0.79	10284	1353	796
	500	25	600			0.6	17140	1781	1048
		30	630			0.62	17140	1724	1014
		35	640			0.59	17140	1811	1065
		40	670			0.62	17140	1724	1014
	700	25	670			0.49	23997	2181	1283
		30	690			0.5	23997	2137	1257
		35	710			0.48	23997	2226	1310
		40	720			0.48	23997	2226	1310

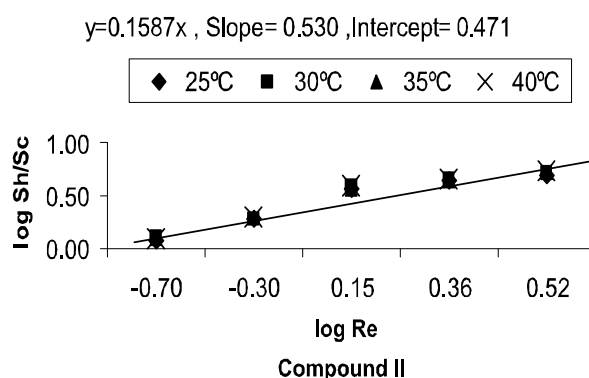
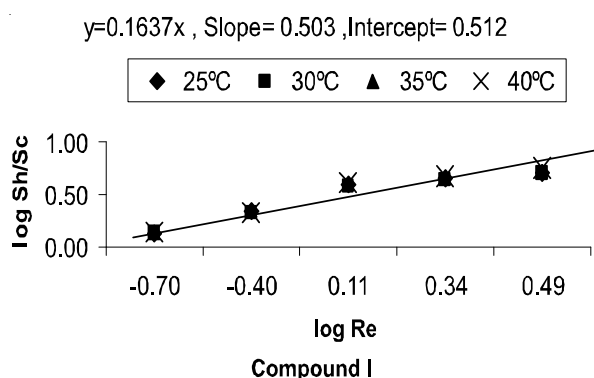


Fig. 10. Overall, mass transfer correlation for all organic compounds at different temperatures

Copper cylinder $Sh = 0.268 Re^{0.7} Sc^{0.33}$
 Steel cylinder $Sh = 0.471 Re^{0.530} Sc^{0.33}$

REFERENCES

1. W. Plieth, *Electrochim. Acta*, **37**, 2115 (1992).
2. E.K. Yung, L.T. Romankiw and R.C. Alkire, *J. Electrochem. Soc.*, **136**, 206 (1989).
3. T.R. Anthony, *J. Appl. Phys.*, **52**, 5340 (1981).
4. P.C. Andricacos, C. Uzoh, J.O. Dukovik, J. Jorkans and H. Deligianni, *IBM J. Res. Dev.*, **42**, 567 (1998).
5. P.C. Andricacos, *Interface*, **1**, 23 (1998).
6. T.P. Moffat, J.E. Bonevich, W. Huber, A. Stanishevsky, D.R. Kelly, G.R. Stafford and D. Josell, *J. Electrochem. Soc.*, **147**, 4524 (2000).
7. A.C. West, S. Mayer and J. Reid, *Electrochem. Solid-State Lett.*, **4**, C50 (2001).
8. M.A. Pasquale, D.P. Barkey and A.J. Arvia, *J. Electrochem. Soc.*, **152**, C149 (2005).
9. P.M. Vereecken, R.A. Binstead, H. Deligianni and P.C. Andricacos, *IBM J. Res. Dev.*, **49**, 3 (2005).
10. D. Josell, D. Wheeler, W.H. Huber and T.P. Moffat, *Phys. Rev. Lett.*, **81**, 016102 (2001).
11. K. Kondo, T. Matsumoto and K. Watanabe, *J. Electrochem. Soc.*, **151**, C250 (2004).
12. A.M. Ahmed, A.A.-H. Abdel-Rahman and A.F. El Adl, *J. Dispers. Sci. Technol.*, **31**, 343 (2010).
13. A.M. Ahmed, A.A.-H. Abdel-Rahman and A.F. El Adl, *J. Dispers. Sci. Technol.*, **32**, 453 (2011).
14. D. Shimkunaite and L. Valentelis, *Chemija (Lithuania)*, **2**, 30 (1991).
15. D. Stoychev, I. Vitanova, R. Bujukliev, N. Etkova, I. Popova and I. Pojarliev, *J. Appl. Electrochem. (London)*, **2**, 978 (1992).
16. D. Josell, D. Wheeler, W.H. Huber and T.P. Moffat, *Electrochem. Solid-State Lett.*, **5**, C49 (2002).
17. Y. Cao, P. Taephaisitphongse, R. Chalupa and C. West, *J. Electrochem. Soc.*, **148**, C466 (2001).
18. F.J. Rodriguez Nieto, M.A. Pasquale, M.E. Martins, F. Barieles and A.J. Arvia, *Monte Carlo Methods Appl.*, **12**, 271 (2006).
19. K. Kondo, N. Yamakawa, Z. Tanaka and K. Hayashi, *J. Electroanal. Chem.*, **559**, 137 (2003).
20. S.-E. Bae and A. Gewirth, *Langmuir*, **22**, 10315 (2006).
21. Y. Jin, K. Kondo, Y. Suzuki, T. Matsumoto and D.P. Barkey, *Electrochem. Solid-State Lett.*, **8**, C6 (2005).
22. D.M. Soares, S. Wasle, K.G. Weil and K. Doblhofer, *J. Electroanal. Chem.*, **532**, 353 (2002).
23. J.J. Kim, S.-K. Kim and Y.S. Kim, *J. Electroanal. Chem.*, **542**, 61 (2003).
24. B. Bozzini, L. D'Urzo, V. Romanello and C. Mele, *J. Electrochem. Soc.*, **153**, C254 (2006).
25. Z.D. Schultz, Z.V. Feng, M.E. Biggin and A. Gewirth, *J. Electrochem. Soc.*, **153**, C97 (2006).
26. W.-P. Dow, H.-Sh. Huang, M.-Y. Yen and H.-H. Chen, *J. Electrochem. Soc.*, **152**, C77 (2005).
27. G.A. Hope and R. Woods, *J. Electrochem. Soc.*, **151**, C550 (2004).
28. B. Bozzini, C. Mele, L. D'Urzo, G. Giovannelli and S. Natali, *J. Appl. Electrochem.*, **36**, 789 (2006).
29. M. Kang and A.A. Gewirth, *J. Electrochem. Soc.*, **150**, C426 (2003).
30. J.P. Healy, D. Pletcher and M. Goodenough, *J. Electroanal. Chem.*, **338**, 155 (1992).
31. J.J. Kelly and A.C. West, *J. Electrochem. Soc.*, **145**, 3472 (1998).
32. V.D. Jovic and B.M. Jovic, *J. Serb. Chem. Soc.*, **66**, 935 (2001).